

## **Autoinduction through the coupling of nucleation-dependent self-assembly of a supramolecular gelator and a reaction network..**

Jamie S. Foster<sup>a</sup> and Gareth O. Lloyd<sup>b\*</sup>

<sup>a</sup> *Institute of Chemical Sciences, School of Engineering and Physical Sciences,  
Heriot-Watt University, Edinburgh, Scotland, United Kingdom, EH14 4AS.*

<sup>b</sup> *Department of Chemistry, School of Natural Sciences, Joseph Banks Laboratories,  
Lincoln, LN6 7DL, United Kingdom.*

*Email: [glloyd@lincoln.ac.uk](mailto:glloyd@lincoln.ac.uk)*

## Table of Contents

<b>1.0 TECHNICAL AND MATERIAL DETAILS .....</b>	<b>3</b>
<b>1.1 POWDER X-RAY DIFFRACTION: .....</b>	<b>3</b>
<b>1.2 NMR SPECTROSCOPY: .....</b>	<b>3</b>
<b>1.3 SEM: .....</b>	<b>3</b>
<b>1.4 IR: .....</b>	<b>3</b>
<b>1.5 HIGH PERFORMANCE LIQUID CHROMATOGRAPHY (HPLC): .....</b>	<b>3</b>
<b>1.6 RHEOLOGY .....</b>	<b>3</b>
<b>2.0 EX SITU PREPARATION OF THE TRIPODAL GELATOR C .....</b>	<b>4</b>
<b>1.1 YIELD .....</b>	<b>4</b>
<b>1.2 <sup>1</sup>H NMR .....</b>	<b>4</b>
<b>1.3 <sup>13</sup>C NMR .....</b>	<b>4</b>
<b>1.4 IR .....</b>	<b>4</b>
<b>1.5 MS .....</b>	<b>4</b>
<b>1.6 MELTING POINT .....</b>	<b>4</b>
<b>3.0 GEL PREPARATION USING EX SITU PREPARED SAMPLE OF C .....</b>	<b>5</b>
<b>4.0 RHEOLOGY OF GEL FORMED WITH EX SITU PREPARED C .....</b>	<b>6</b>
<b>5.0 AVRAMI COEFFICIENT DETERMINATION FOR GEL FORMED WITH EX SITU PREPARED C .....</b>	<b>7</b>
<b>6.0 SEM IMAGE OF GEL PREPARED WITH EX SITU SYNTHESISED .....</b>	<b>8</b>
<b>6.0 IR EVIDENCE FOR REACTION WITH AROMATIC –NH<sub>2</sub> .....</b>	<b>9</b>
<b>7.0 IN SITU FORMATION OF C AND SUBSEQUENT HYDROGEL FORMATION .....</b>	<b>10</b>
<b>8.0 CONTROL OF MECHANICAL PROPERTIES THROUGH CHEMICAL REACTION .....</b>	<b>11</b>
<b>9.0 DETERMINED CHEMICAL REACTION KINETIC DATA FOR ALL TECHNIQUES .....</b>	<b>12</b>
<b>10.0 IN SITU FORMATION OF C<sup>N</sup>- WITH ADDITION OF C<sup>N</sup>- SEED .....</b>	<b>14</b>
<b>11.0 REACTION ORDER DETERMINATION .....</b>	<b>16</b>
<b>12.0 IN SITU FORMATION OF C<sup>N</sup>- WITH MECHANICAL AGITATION .....</b>	<b>19</b>
<b>13.0 STANDARD VS SEEDING VS MECHANICAL REACTION CONDITIONS RATE OF REACTION .....</b>	<b>22</b>
<b>14.0 MOLAR ABSORPTIVITY DETERMINATION FOR A AND C .....</b>	<b>23</b>
<b>14.2 MOLAR ABSORPTIVITY DETERMINATION FOR C .....</b>	<b>24</b>
<b>15.0 HPLC CHROMATOGRAMS FOR A AND C .....</b>	<b>25</b>
<b>16.0 HPLC DATA FOR C<sup>N</sup>- FORMATION (STANDARD CONDITIONS) .....</b>	<b>26</b>
<b>17.0 PXRD PATTERNS FOR DRIED GEL SAMPLES .....</b>	<b>27</b>

## 1.0 Technical and material details

### 1.1 Powder X-Ray Diffraction:

PXRD patterns were collected at room temperature using a Bruker D8 Advance powder diffractometer in reflectance mode. Lynxeye super speed detector was used with the radiation being monochromated Cu K $\alpha$ 1, with a characteristic wavelength of 1.541 Å. 30 minute scans over the range  $5^\circ \leq 2\theta \leq 60^\circ$  (stepsize = 0.014481°/counting time = 0.5 s/steps).

### 1.2 NMR spectroscopy:

NMR spectra were recorded on a Bruker AV 400 operating at 400.1 MHz for  $^1\text{H}$  and 100.6 MHz for  $^{13}\text{C}$  experiments.

### 1.3 SEM:

SEM images were produced using a Philips XL30 LaB6 ESEM equipped with an Oxford Instrument X-max 80 EDX detector. A thin layer gold coating was applied to samples before imaging.

### 1.4 IR:

IR spectra were recorded on a Nicolet is5 instrument using 24 scans at a resolution of  $1\text{ cm}^{-1}$  and data spacing of  $0.964\text{ cm}^{-1}$ .

### 1.5 High performance liquid chromatography (HPLC):

Chromatography carried out at UV detection at 290 nm using a Shimadzu HPLC with a Thermo Scientific Accucore C18 column (100 x 4.6 mm, particle size of  $\mu\text{ 2.6}$ ). Flow rate 0.8 mL/min using 100 % methanol.

### 1.6 Rheology

Rheological experiments were performed on a Bohlin nano II rheometer. A 40 mm aluminium plate was used with an operating gap of 300  $\mu\text{m}$  gap and a solvent trap. For all gels 5 ml of the solution was prepared and added to the plate with a syringe in the operating gap so the gel could form in contact with the cone.

Time sweep experiments were commenced immediately upon addition of the solutions. All samples were recorded over 15 h at 20 °C with a torque of 100  $\mu\text{Nm}$  and a frequency of 10 Hz, data was taken every 30 s for a sample time of 3 s.

Frequency sweep experiments were performed immediately after the time sweep at 20 °C. The torque was kept constant at 100  $\mu\text{Nm}$ .

Stress sweep experiments were recorded after frequency sweep experiments. All samples were recorded at 20 °C and at a frequency of 1 Hz.

## 2.0 *Ex situ* preparation of the tripodal gelator C

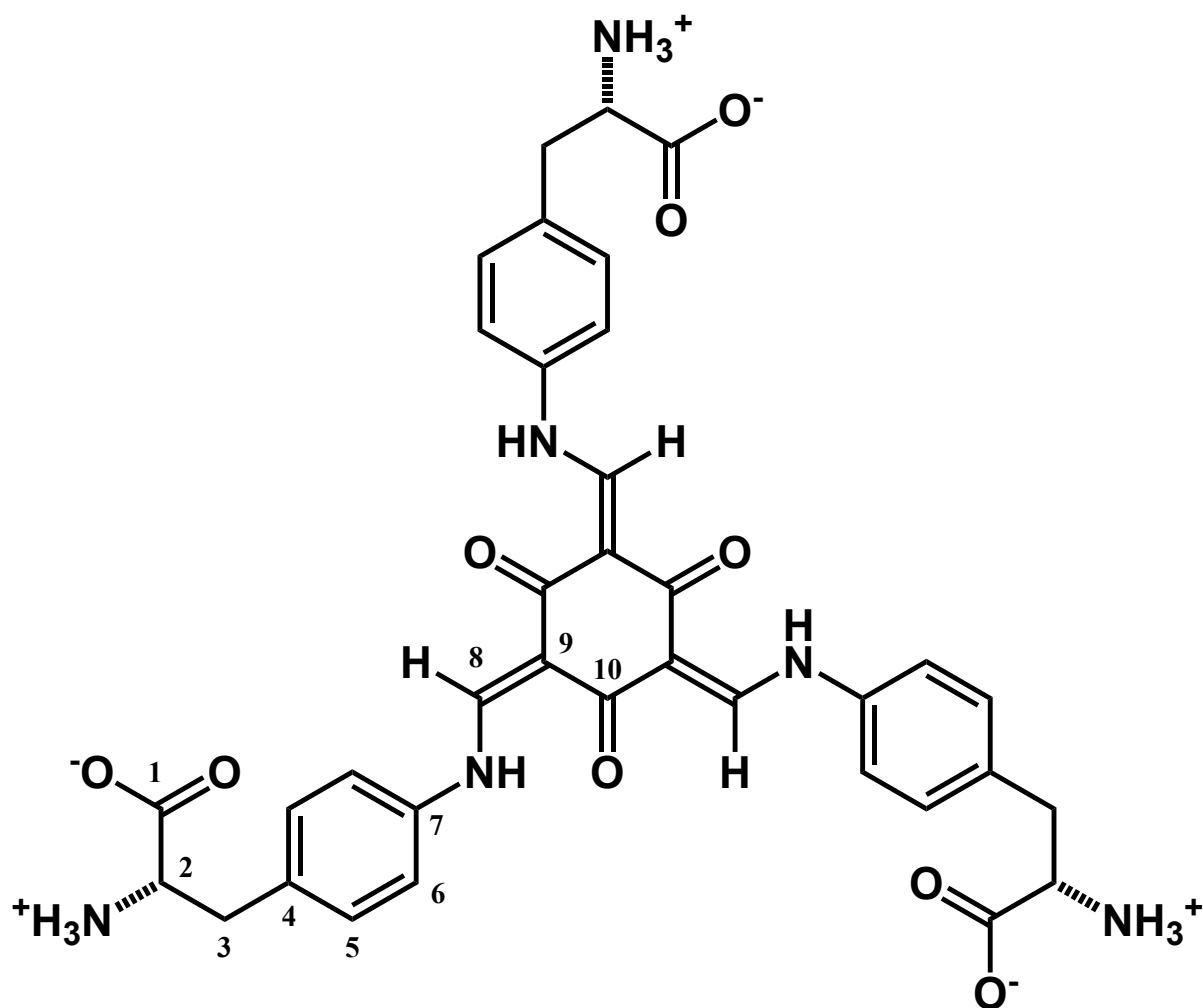


**Figure S1.** Chemical structure of the *ex situ* prepared tripodal, tri-amino acid gelator (2*S*,2'*S*,2''*S*)-3,3',3''-(((1*E*,1'*E*,1''*E*)-(2,4,6-trioxocyclohexane-1,3,5-triylidene)tris(methanoylidene))tris(azanediyl))tris(benzene-4,1-diyl))tris(2-aminopropanoic acid) (**C**) (numbers are used for the <sup>13</sup>C assignment).

To a mixture of 1,3,5-triformylphloroglucinol (**A**) (0.25 g, 1.19 mmol, 1 equiv.) and 4-amino-*L*-phenylalanine (0.66 g, 3.69 mmol, 3.1 equiv.) ethanol (50 ml) was added. The resulting suspension was brought to reflux and the reaction allowed to proceed for 24 hours, this produced a bright yellow suspension. The reaction mixture was allowed to cool to room temperature before the product was collected by vacuum filtration. The resulting yellow solid was then washed with water (5 x 50 ml) before being collected and dried in an oven overnight (80 °C) to yield the final product in good purity and yield.

**1.1** Yield: 91 %, 0.75 g, (M.W. = 696.25 gmol<sup>-1</sup>)

**1.2** <sup>1</sup>H NMR (D<sub>2</sub>O + NaOH J/Hz, δ/ppm): 7.51 (s, 3H, =CH-), 7.48 (dd, J = 75.21, 8.08, 12H, Ar-H), 3.92 (dd, J = 7.89, 5.3, 6H, -CH<sub>2</sub>-), 3.15 (m, 3H, -CH-NH<sub>2</sub>)\*.

**1.3** <sup>13</sup>C NMR (D<sub>2</sub>O + NaOH J/Hz, δ/ppm): 187.21 (10), 179.11 (1), 169.03 (8), 144.59 (7), 130.66 (5), 130.31 (9), 129.41 (4), 116.72 (6), 59.98 (2), 38.07 (3).

**1.4** IR (cm<sup>-1</sup>): 3334, 2859, 1598, 1515, 1411, 1361, 1314, 1269, 1041, 839, 742, 711, 651, 611, 584.

**1.5** MS HRMS (ESI<sup>-</sup>): calculated for [M-H]<sup>-</sup> 695.2507, C<sub>36</sub>H<sub>35</sub>N<sub>6</sub>O<sub>9</sub> found: 695.2471.

**1.6** Melting point: Decomposes upon heating (> 300 °C).

\* The use of D<sub>2</sub>O + NaOH as the NMR solvent due to the insolubility of **C** all -NH<sub>x</sub> and -OH <sup>1</sup>H signals are lost through deuterium exchange and deprotonation.

### 3.0 Gel preparation using *ex situ* prepared sample of **C**

Typical gelation: **C** (0.075 g, 0.108 mmol) was added to water (3 ml) to create a suspension. To this suspension solid NaOH was slowly added until **C** had completely dissolved and the solution had reached a pH of 8.5. To this solution glucono-delta-lactone (GdL) (0.170 g, 0.972 mmol, 9 equivalents relative to **C**) was added and the solution shaken until the GdL had fully dissolved. The solution was allowed to rest at room temperature resulting in the formation of a gel after 20 minutes.

Critical gelation concentration (CGC) = 0.5 wt%, 7.18 mmolL<sup>-1</sup>.

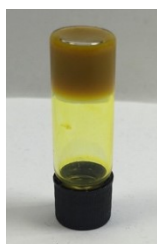


**Figure S2.** Photograph of gel formed using *ex situ* prepared sample of **C** (0.075 g, 0.108 mmol) gelling water (3 ml) to make a gel (2.5 wt%).

## 4.0 Rheology of gel formed with *ex situ* prepared C

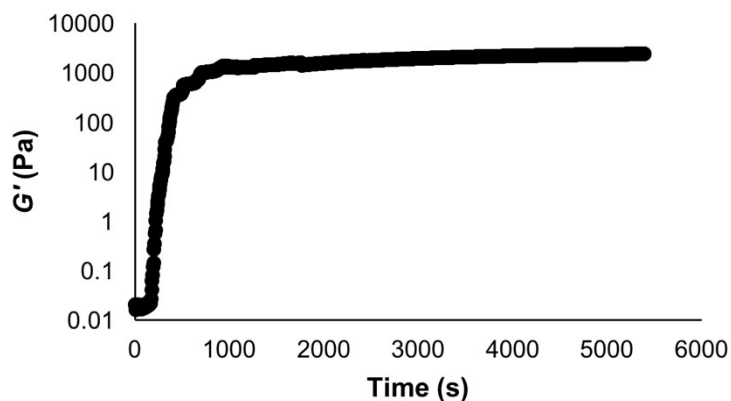


**Figure S3.** Time sweep rheometry of gel prepared using *ex situ* synthesized C. Storage modulus  $G'$  (Pa) (y-axis) plotted (log scale) against time (s) (x-axis).

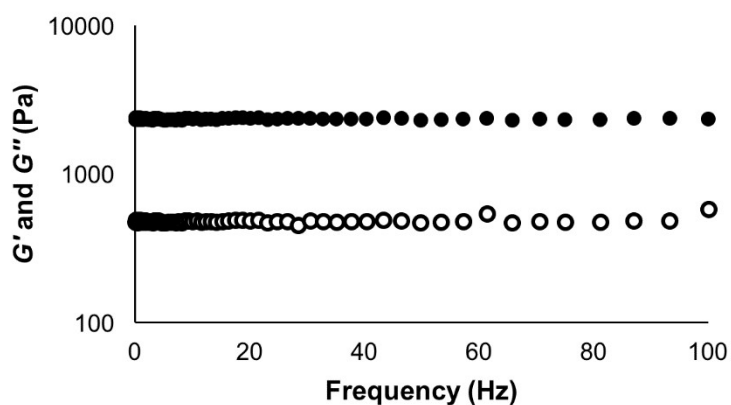


**Figure S4.** Frequency sweep rheometry of gel prepared using *ex situ* synthesized C. The storage modulus  $G'$  (Pa) (blue) and the loss modulus  $G''$  (Pa) (red) are shown as a log scale (y-axis) against the frequency (Hz) (x-axis).

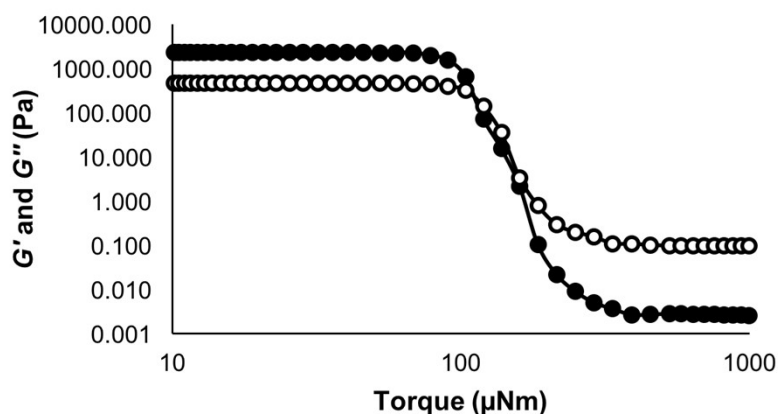


**Figure S5.** Amplitude sweep rheometry of gel  $C_k$  prepared using *ex situ* synthesized C. The storage modulus  $G'$  (Pa) (y-axis) plotted against torque ( $\mu\text{Nm}$ ) (x-axis) shown in a log scale. A line between data points added to guide the eye.

## 5.0 Avrami coefficient determination for gel formed with *ex situ* prepared C

The Avrami coefficient ( $n$ ) could be determined by plotting  $\ln(-\ln(1-X))$ , where  $X = (G'_t - G'_0) / (G'_\infty - G'_0)$  ( $G'_t = G'$  at time  $t$ ,  $G'_0 = G'$  at time = 0,  $G'_\infty = G'$  average of last 5 data points) against  $\ln(t - t_0)$ . The Avrami constant is the first part of the slope where the nucleation process begins.

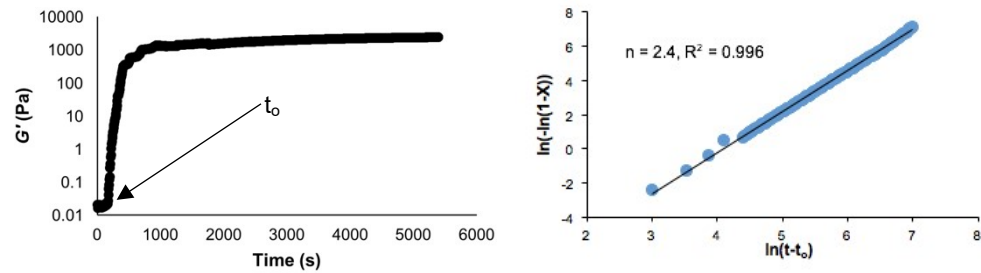


**Figure S6.** Time sweep rheology experiment (right) and the derived Avrami plot (left) of gel prepared using *ex situ* synthesized C.

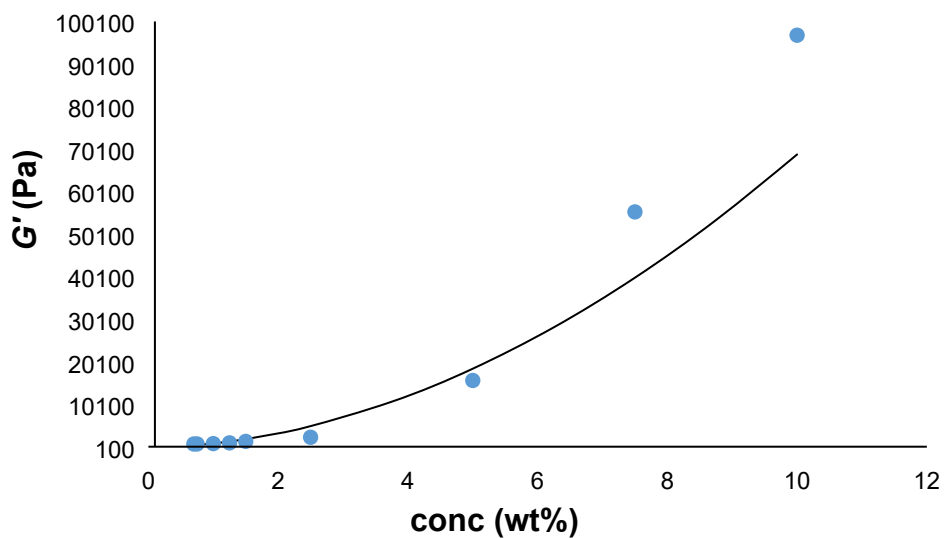


**Figure S7.** Study in the variation in  $G'$  with changing concentration for gels formed with varying amounts of *ex situ* prepared C.

## 6.0 SEM image of gel prepared with *ex situ* synthesised

Gel samples were placed on carbon covered aluminium SEM stubs and dried for seven days under vacuum. The resulting xerogel was gold coated and SEM images were obtained from the samples.

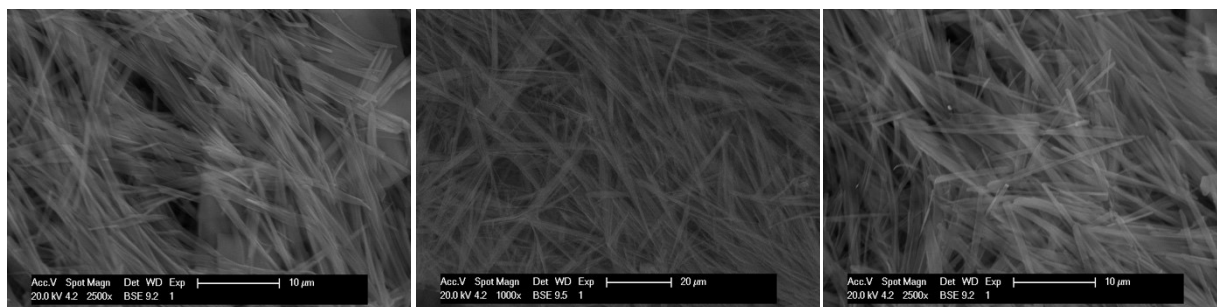


**Figure S8.** SEM image of dried gel made using *ex situ* prepared sample of **C**. Visible are fibres that arise from the supramolecular assembly of the individual molecules of **C** that ultimately immobilize the water.

## 6.0 IR evidence for reaction with aromatic –NH<sub>2</sub>

There are two possible amines with which the aldehyde groups of **A** can react, the aromatic NH<sub>2</sub>s and the NH<sub>2</sub> groups associated with the amino acid groups. IR and <sup>13</sup>C NMR analysis of **C** have shown that imine/enamine formation occurs only at the aromatic –NH<sub>2</sub> group.

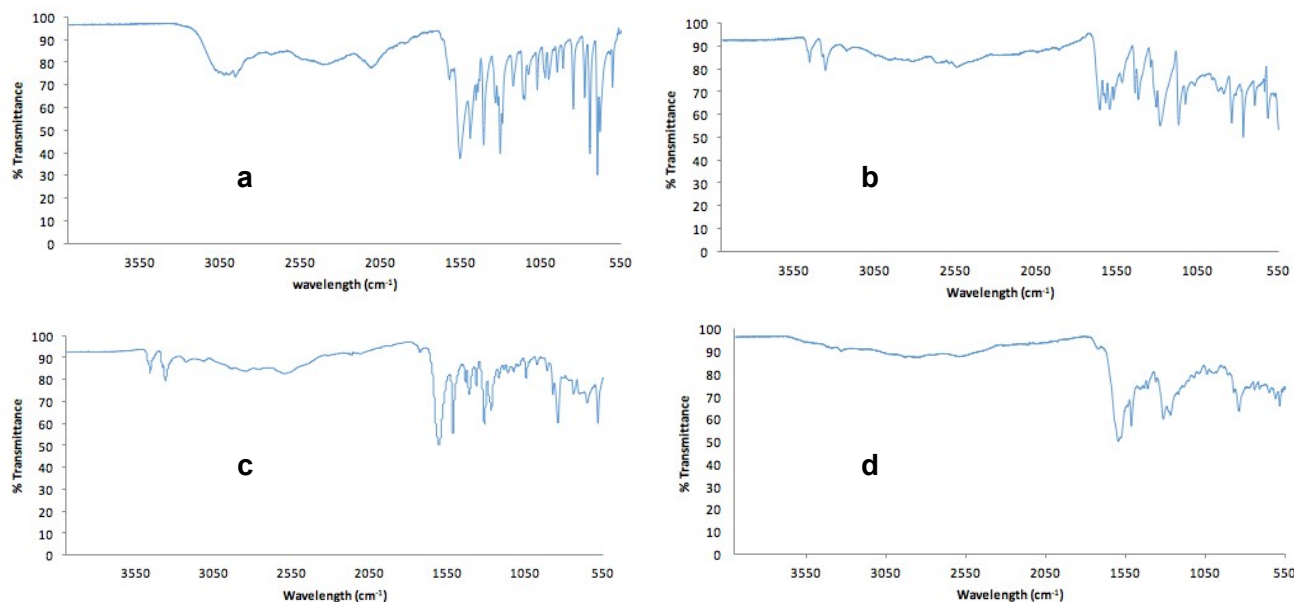


**Figure S9.** IR spectra showing *L*-phenylalanine (a), 4-aminobenzoic acid (b), 4-amino-*L*-phenylalanine (c), **C** (d).

The peaks associated with the Ar-NH<sub>2</sub> group (twin peaks ~3400 cm<sup>-1</sup> are visible in spectra (b) and (c) but not in (d). This shows the reaction likely occurs at the Ar-NH<sub>2</sub> group of 4-amino-*L*-phenylalanine. The NH<sub>3</sub><sup>+</sup> vibrational peaks of amino acids are normally very broad (around 3100 cm<sup>-1</sup>) and are not clearly visible in these samples nor is the acidic N-H of the product ketoenamine.

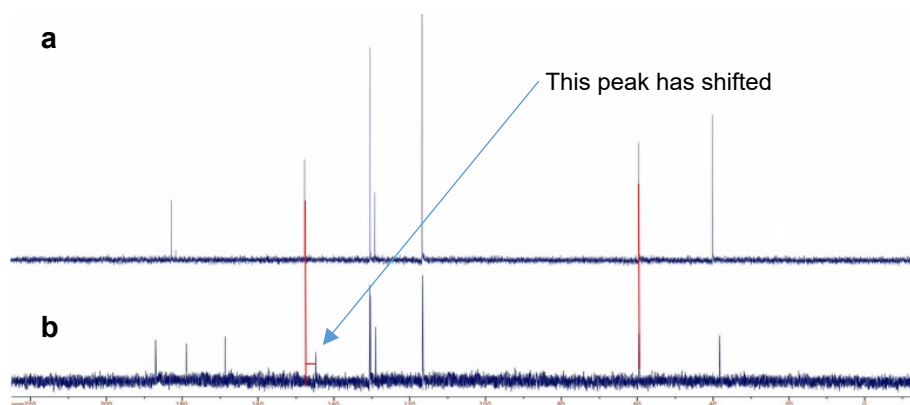


**Figure S10.**  
<sup>13</sup>C NMR  
spectra for

4-amino-l-phenylalanine (a) and **C**<sup>n-</sup> (b) with red lines highlighting carbons adjacent to amine groups.

There is a consistent 2.5 ppm shift in the signal of the carbon associated with the Ar-NH<sub>2</sub> group when comparing the spectra for **A** and **C** while the carbon signal for the amino acid C-NH<sub>2</sub> shows no shift. This can be attributed to the reaction at the Ar-NH<sub>2</sub> and the subsequent conversion into an enamine.

## 7.0 *In situ* formation of **C** and subsequent hydrogel formation

The reaction of 4-aminophenylalanine and 1,3,5-triformylglucinol at pH 8.5 in water yielded **C** after several days in a stoichiometric yield. The typical procedure for such a reaction is as follows:

1,3,5-trifluoroglucinol (0.0294 g, 0.14 mmol, 1 equiv) was suspended in water (2.5 ml) while 4-aminophenylalanine (0.0756 g, 0.42 mmol, 3 equiv) was dissolved in a separate portion of water (2.5 ml). These solutions were mixed together and the pH of the combined solution was adjusted to pH 8.5 with the addition of solid NaOH while ensuring the complete dissolution of the 1,3,5-triformylglucinol. After a period of 72 hours complete conversion to **C** had occurred.

Direct addition of GdL to the solution after 72 hours (0.30 g, 1.68 mmol, 12 equiv.) will result in the formation of a gel with comparable mechanical strength to a gel prepared using *ex situ* synthesized **C**.

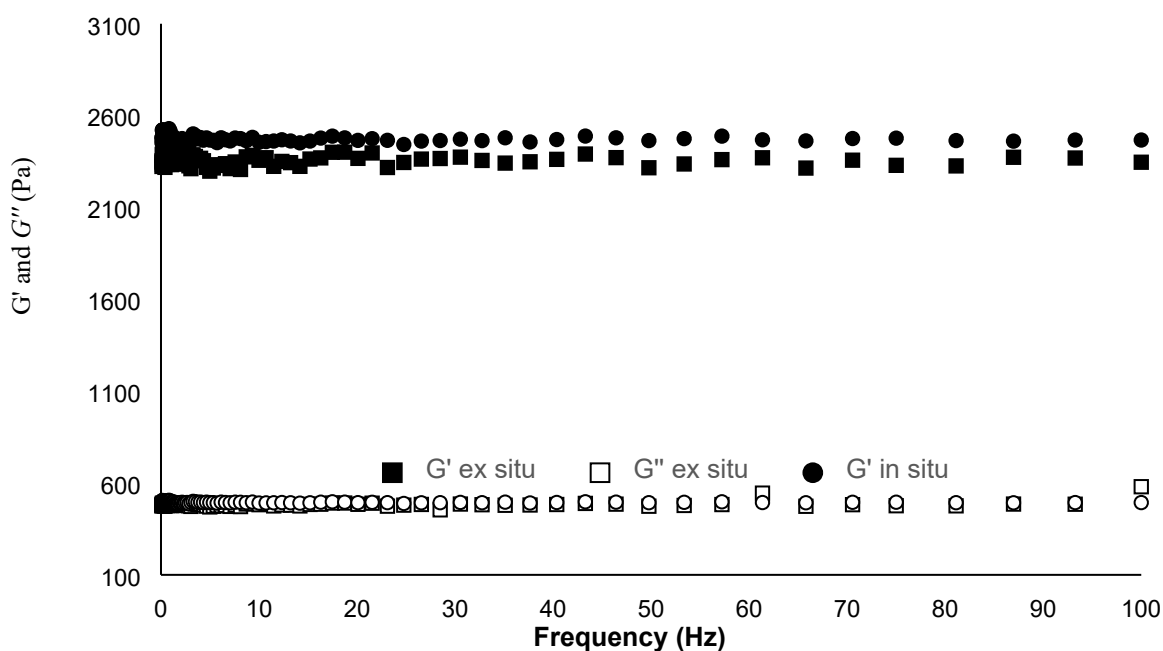
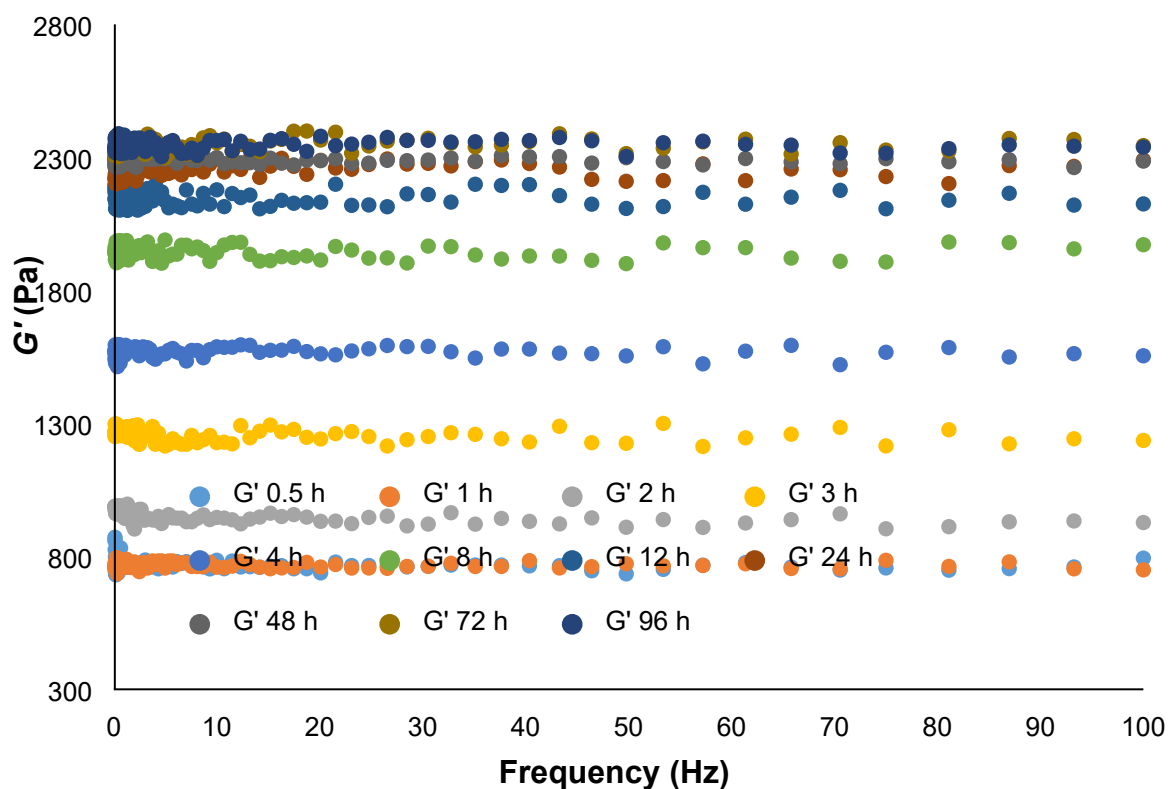


Figure S11. Comparison mechanical strength of *ex situ* and *in situ* (72-hour reaction time) gels

## 8.0 Control of mechanical properties through chemical reaction

The utilization of the time taken for the *in situ* reaction of **A** and **B** to **C** to go to completion and the ability of **C** to form a supramolecular gel results in the ability to stop the reaction through a mass transfer limitation mechanism. This ‘freezing’ of the reaction results in a lower concentration of **C** which in turn results in a mechanical weaker gel.



**Figure S12.** Frequency sweep experiments ( $G'$  shown only for clarity) for the gels resulting from the set using a 2 ml portion of a 25 ml stock solution with a potential maximum **C** of  $28.2 \text{ mmol}^{-1}$ .

## 9.0 Determined chemical reaction kinetic data for all techniques

The conversion of **A + B** to **C<sup>n</sup>** was monitored in terms of increasing concentration of the product **C<sup>n</sup>** which could be determined by rheology with use of the cellular solid model which predicts a relationship of  $G' \propto [\text{conc}]^2$  see figure. S7. The increasing concentration of **C<sup>n</sup>** was also monitored using <sup>1</sup>H NMR, UV-vis spectroscopy and HPLC – UV-vis spectroscopy.

**Table S1.** Raw data for the increasing concentration of reaction product **C<sup>n</sup>** with time. Measured and calculated with rheology, <sup>1</sup>H NMR, UV-vis and HPLC-UV-vis.

Time (hours)	conc. from rheology (mM).	Conc. from NMR (mM).	Conc. from UV-vis (mM).	Conc. from HPLC (mM).
0.5	13.15	7.9	6.23	7.78
1	13.52	8.07	6.31	7.72
2	14.73	9.32	7.28	9.22
3	17.23	12.05	9.58	11.82
4	19.53	14.67	12.77	14.32
8	21.71	19.66	18.43	19.93
12	22.93	23.81	22.48	23.58
24	23.50	26.36	24.78	26.53
48	24.04	27.72	25.92	27.49
72	24.08	28.0	26.11	27.95
96	24.03	28.0	26.13	27.87

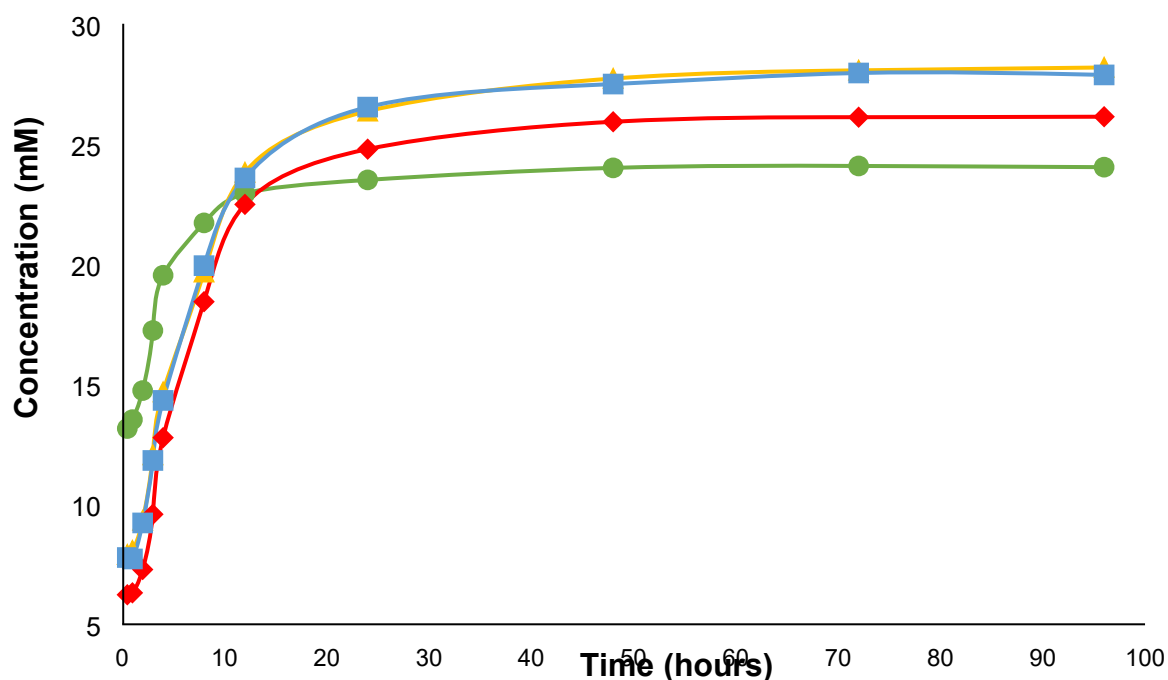


**Figure S13.** Concentration (in mM) of reaction product **C<sup>n</sup>** monitored over time by rheology (green ●), <sup>1</sup>H NMR (yellow ▲), UV-vis (red ◆) and HPLC (blue ■) against time (hours, log scale) with a line added between data points to guide the eye.

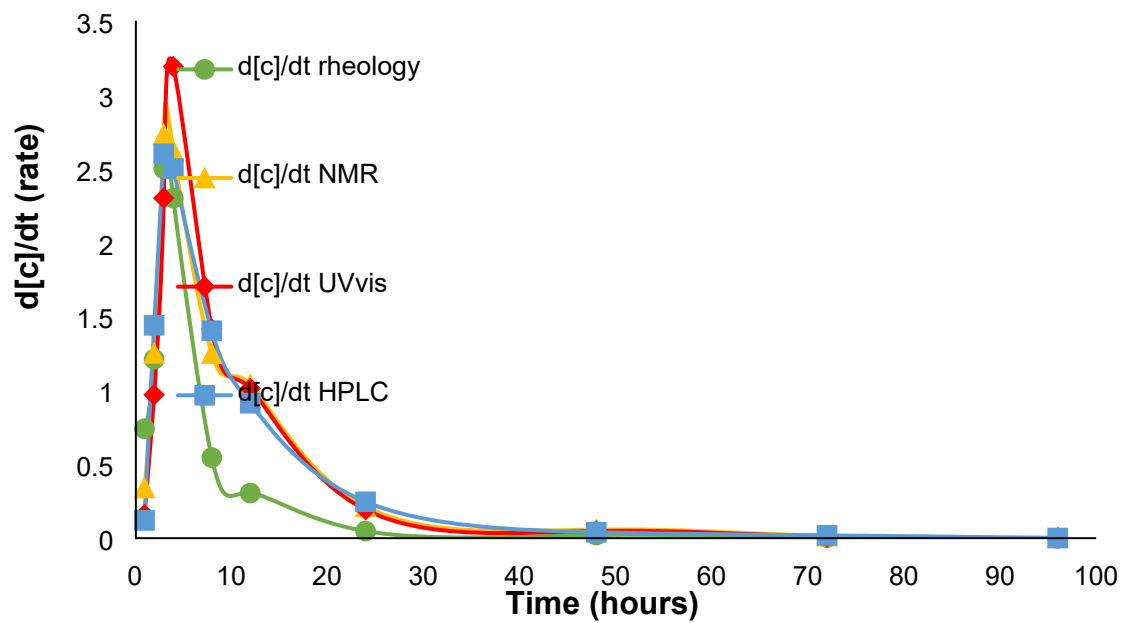


**Figure S14.** The rate of reaction of  $A + B = C^n$  calculated using the previously determined concentration from the by rheology (green ●),  $^1H$  NMR (yellow ▲), UV-vis (red ◆) and HPLC (blue ■) against time (hours, log scale) with a line added between data points to guide the eye.

## 10.0 *In situ* formation of $C^{n-}$ with addition of $C^{n-}$ seed

*Ex situ* prepared  $C^{n-}$  could be added to the *in situ* method for preparing  $C^{n-}$ , this seeding experiment provides the catalytic sites required for the formation of  $C^{n-}$  as soon as **A** and **B** are mixed. This offers confirmation of the autocatalytic kinetic nature of this system.

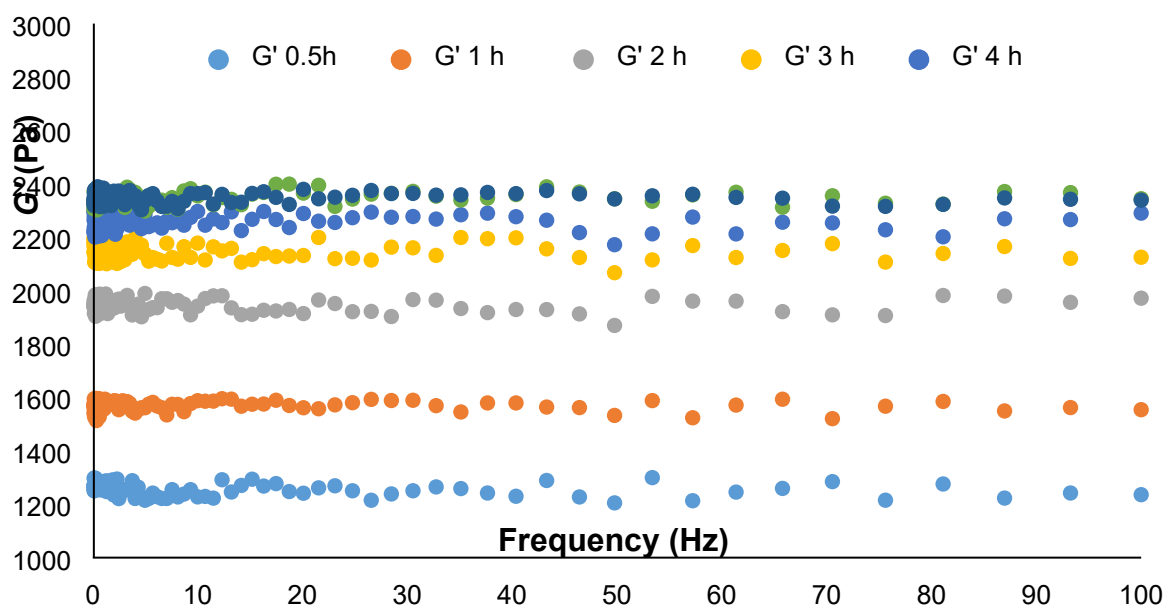


**Figure S15.** Frequency sweep experiments ( $G'$  shown) for the gels resulting from the set using a 2 ml portion of a 25 ml stock solution with a potential maximum  $C$  of  $28 \text{ mmol}^{-1}$ .

**Table S2.** Raw data for the increasing concentration of reaction product  $C^{n-}$  with time. Measured and calculated with rheology,  $^1\text{H}$  NMR and HPLC-UV-vis.

time (hours)	conc. from rheology (mM).	Conc. from HPLC (mM).	Conc. from NMR (mM).
0.5	17.13	8.72	8.65
1	19.39	10.47	10.25
2	21.54	15.88	14.67
3	22.69	21.73	21.04
4	23.27	24.65	25.07
8	24.20	26.94	27.45
12	24.25	27.98	28.03
24	24.27	28.01	28.12

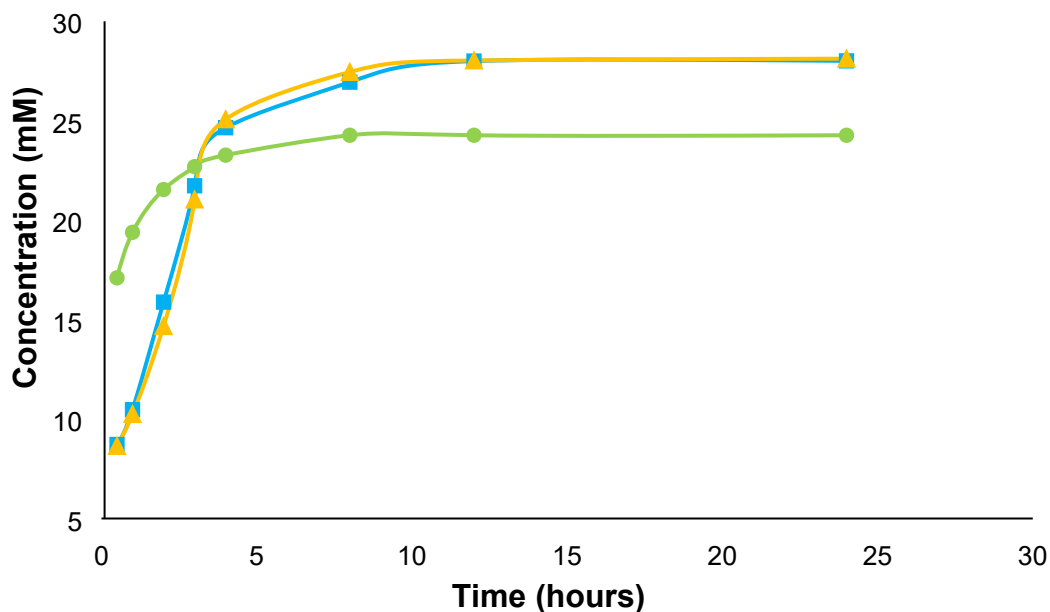


**Figure S16.** Concentration (in mM) of reaction product  $C^{n-}$  formed with a seed concentration of 1.5 mM, monitored over time by rheology (green ●),  $^1\text{H}$  NMR (yellow ▲) and HPLC (blue ■) against time (hours, log scale) with a line added between data points to guide the eye.

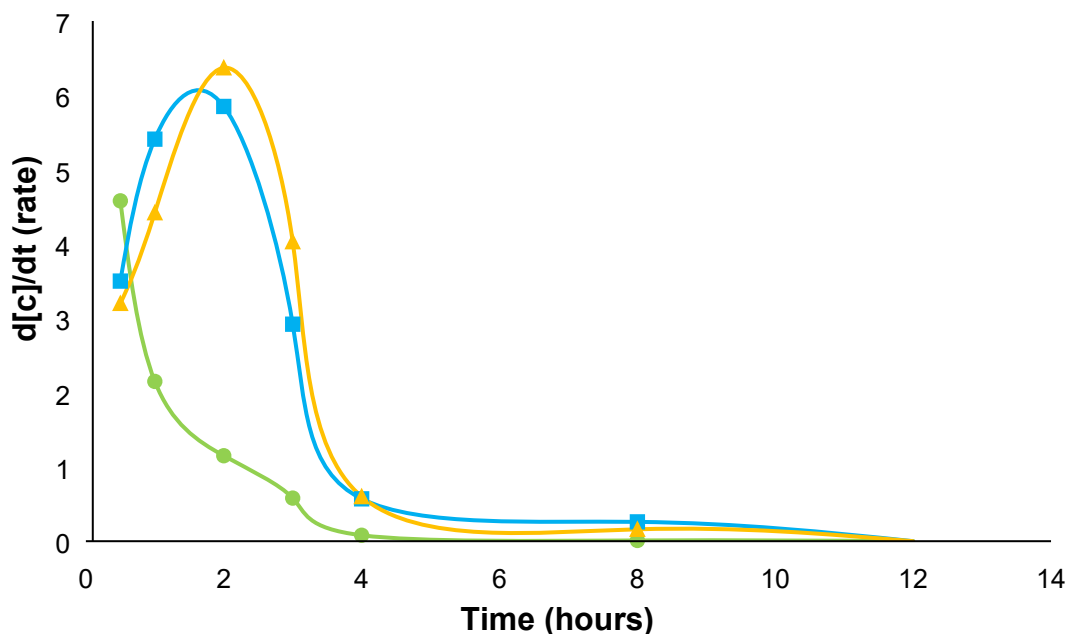


**Figure S17.** The rate of reaction of  $A + B$  to  $C^{n-}$  calculated using the previously determined concentration from the by rheology (green ●),  $^1\text{H}$  NMR (yellow ▲) and HPLC (blue ■) against time (hours, log scale) with a line added between data points to guide the eye.

Concentrations and rates determined from rheology experiments do not appear to show the characteristics of the autocatalytic effect associated with the system. This can be explained by the addition of GdL and the resulting production of gluconic acid. The presence of  $\text{H}^+$  can catalysis the imine bond formation resulting in curves that do not appear to follow the expected sigmoidal profile.

## 11.0 Reaction order determination

Determination of order of reaction in terms of autocatalytic **C** could be achieved using seeding experiments where by previously synthesized **C** could be added into an *in situ* reaction mixture between **A** and **B** as soon as mixing had occurred. Autocatalytic systems will generally have an order in terms of the catalytic addition increasing initial catalytic rates and this determination provides further evidence of the self-replication kinetics and mechanism.

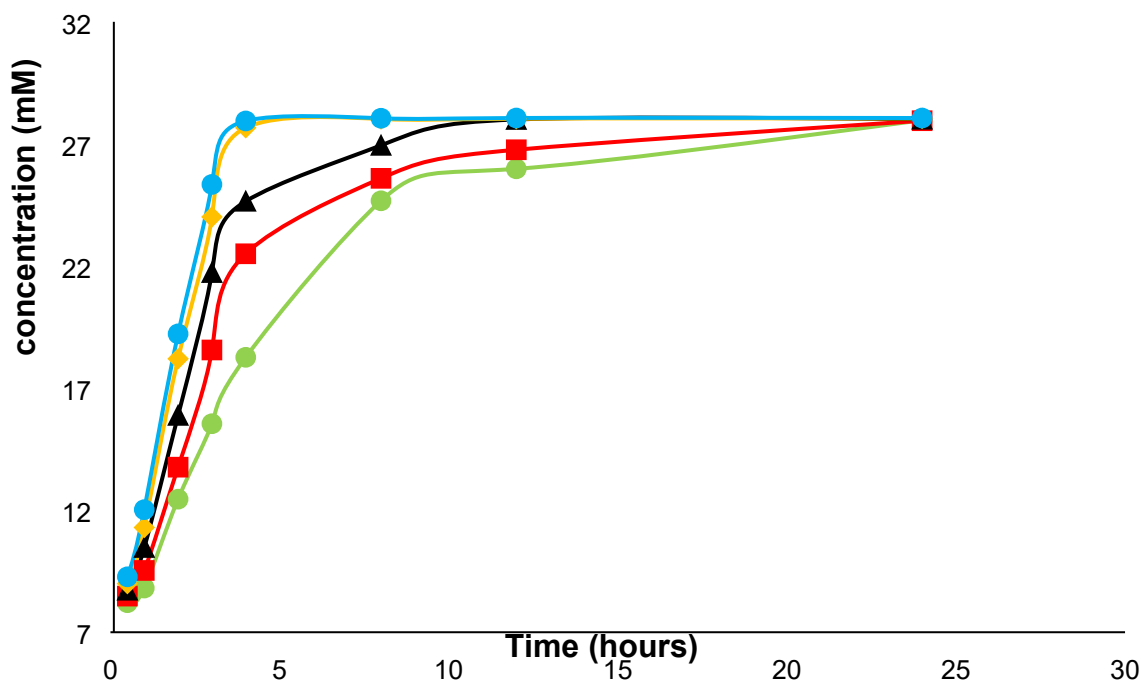


**Figure S18.** Total concentration of  $C^{n-}$  formed over time with different quantities of  $C^{n-}$  added as a seed at time 0 h.  $C_{\text{catalyst}} = 0.5$  mM (green ●),  $C_{\text{catalyst}} = 1.0$  mM (red ■),  $C_{\text{catalyst}} = 1.5$  mM (black ▲),  $C_{\text{catalyst}} = 2.0$  mM (yellow ◆) and  $C_{\text{catalyst}} = 2.5$  mM (blue ●).

**Table S3.** Concentration over time of **C** in solution with varying seed quantities (all concentrations in mM).

time (hours)	[C] (seed = 0.5)	[C] (seed = 1.0)	[C] (seed = 1.5)	[C] (seed = 2.0)	[C] (seed = 2.5)
0.5	8.21	8.48	8.72	8.99	9.27
1	8.81	9.53	10.47	11.29	12.02
2	12.45	13.76	15.88	18.2	19.22
3	15.54	18.56	21.73	24.01	25.34
4	18.26	22.5	24.65	27.66	27.94
8	24.67	25.59	26.94	28.02	28.05
12	25.98	26.76	28.00	28.03	28.06
24	27.97	27.95	28.01	28.04	28.06

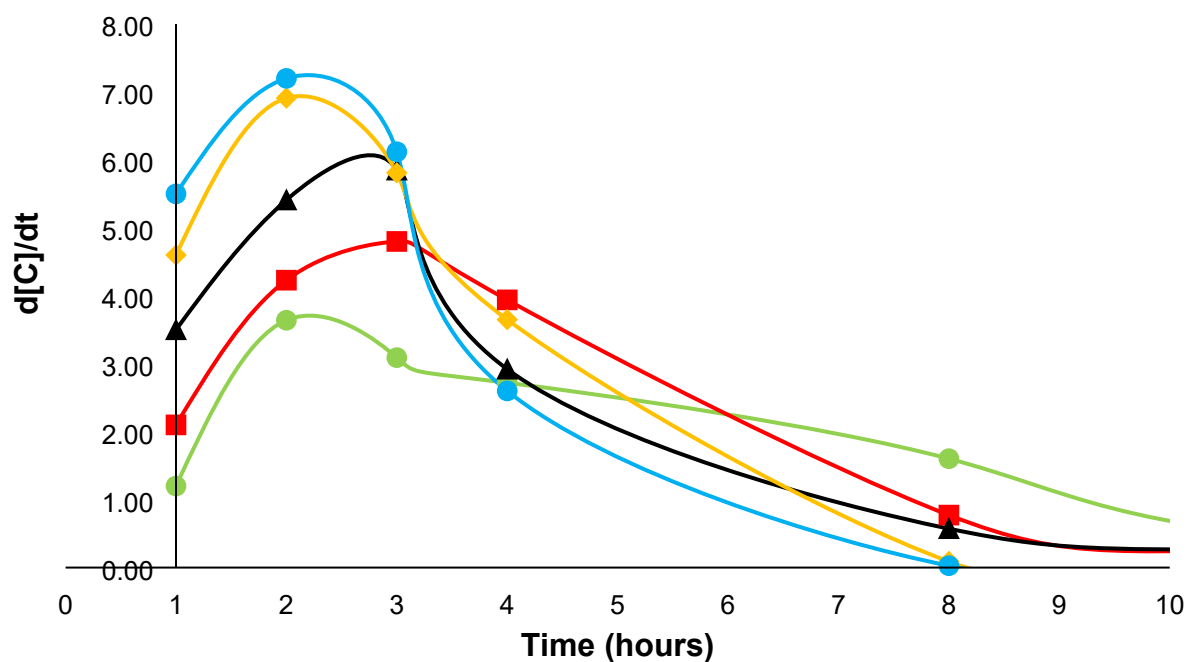


**Figure S19.** Rate ( $d[C]/dt$ ) for the formation of **C** with varying concentration of  $C_{\text{catalyst}}$  added to the reaction mixture at time = 0 h.  $C_{\text{catalyst}} = 0.5$  mM (green ●),  $C_{\text{catalyst}} = 1.0$  mM (red ■),  $C_{\text{catalyst}} = 1.5$  mM (black ▲),  $C_{\text{catalyst}} = 2.0$  mM (yellow ◆) and  $C_{\text{catalyst}} = 2.5$  mM (blue ●).

**Table S4.** Concentration over time of **C** in solution with varying seed quantities (all concentrations in mM).

time (hours)	$d[C]/dt$ (seed = 0.5)	$d[C]/dt$ (seed = 1.0)	$d[C]/dt$ (seed = 1.5)	$d[C]/dt$ (seed = 2.0)	$d[C]/dt$ (seed = 2.5)
1	1.20	2.10	3.50	4.60	5.50
2	3.64	4.23	5.41	6.91	7.20
3	3.09	4.80	5.85	5.81	6.12
4	2.72	3.94	2.92	3.65	2.60
8	1.60	0.77	0.57	0.09	0.03
12	0.33	0.29	0.27	0.00	0.00
24	0.17	0.10	0.00	0.00	0.00

To determine the reaction order in terms of autocatalytic component,  $C^{n-}$  we used the previously determined reaction rates for the different seeding concentrations and plotted the initial rate of  $C^{n-}$  formation (replication) ( $\log d[C^{n-}]/dt$ ) against the concentration of the seed  $C^{n-}$  ( $\log [C^{n-}]$ ).

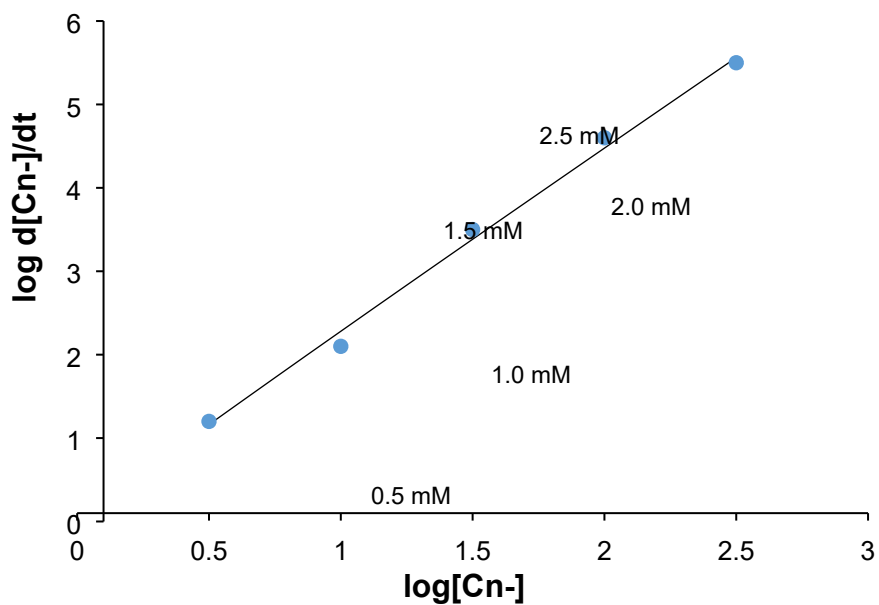


**Figure S20.** Determination of the reaction order for  $A + B \rightarrow C^{n-}$  where  $y = mx^p$  with  $p$  being equal to the order of the reaction (concentrations of seed  $C^{n-}$  marked on graph).

## 12.0 *In situ* formation of $C^{n-}$ with mechanical agitation

A template-based autocatalytic mechanism through some form of interaction of the reactants or intermediates with the product  $C$  is significantly unlikely. The growth of in solution supramolecular polymers during the *in situ* formation of  $C$  acts as a limiting factor in this template catalytic mechanism as propagation of these fibres in terms of their length does not result in an increase in the overall number of catalytic sites as there are only two sites per supramolecular polymer (one at each end). Mechanical agitation or convection induced sheering of the *in situ* reaction mixture will result in the breaking up of the supramolecular polymers, increasing the number of “catalytic sites” thus increasing the rate of reaction for the production of  $C$  from  $A$  and  $B$  through the autoinduction autocatalytic mechanism.

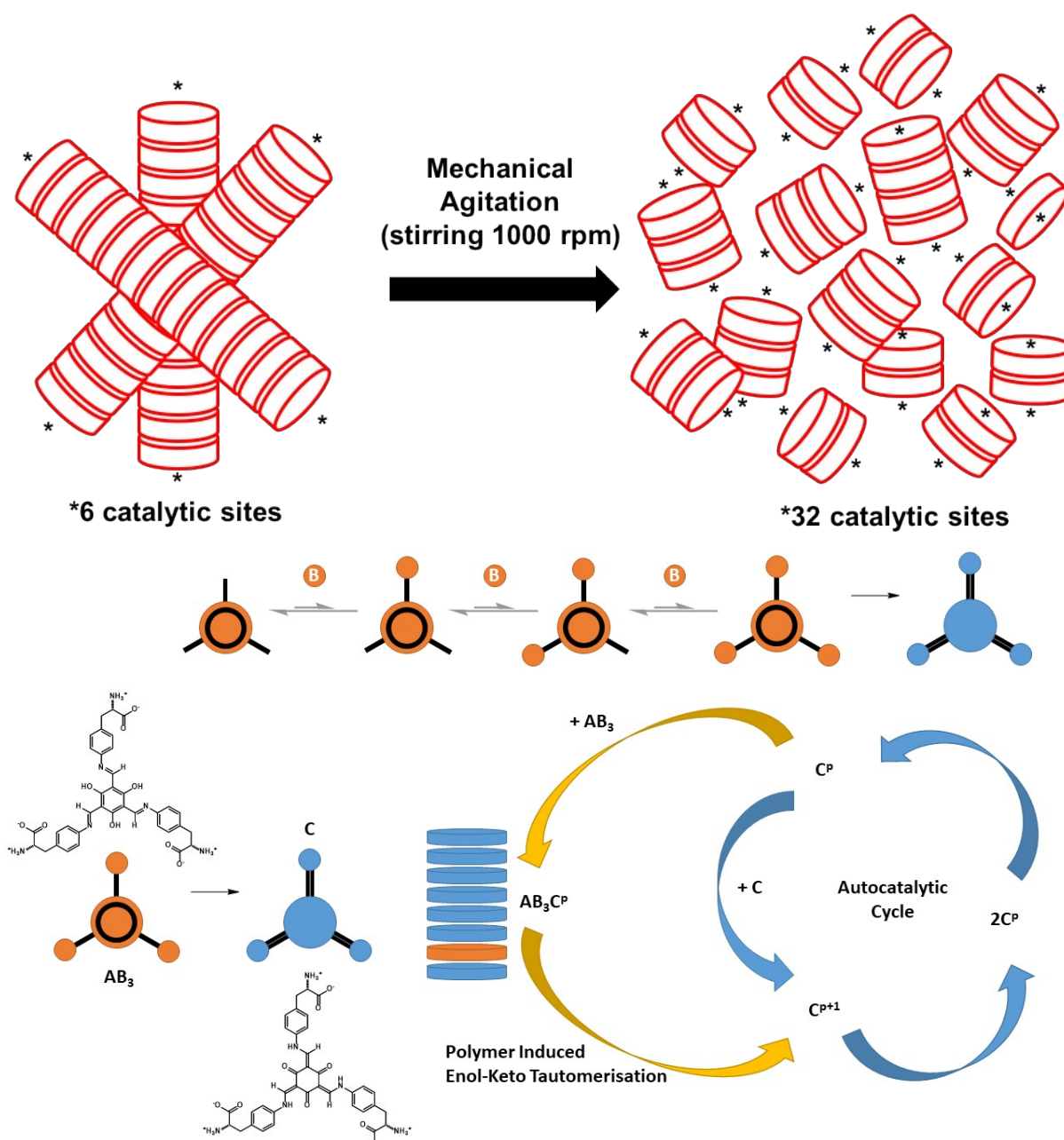


**Figure S21.** Pictorial representation of the effects of mechanical agitation on the supramolecular fibres formed in aqueous conditions (20 °C without mechanical agitation) by the anionic species of  $C$ ,  $C^{n-}$ , and the subsequent increase in the number of “catalytic sites”. These “catalytic sites” can simple be the sites of inclusion of the intermediates of the reaction, in particularly, the enol intermediate  $AB_3$ , which is chemically similar enough to the product to be easily visualized as being capable of forming a coassembled supramolecular polymer.

Evidence of  $C^{n-}$  forming supramolecular fibres in solution was apparent by analysis of the viscosity of the solutions containing different concentrations of  $C^{n-}$  and comparing these concentrations to that of pure water. There is also evidence of the breakdown of the supramolecular polymers at approximately 32 °C (Figure S22.).

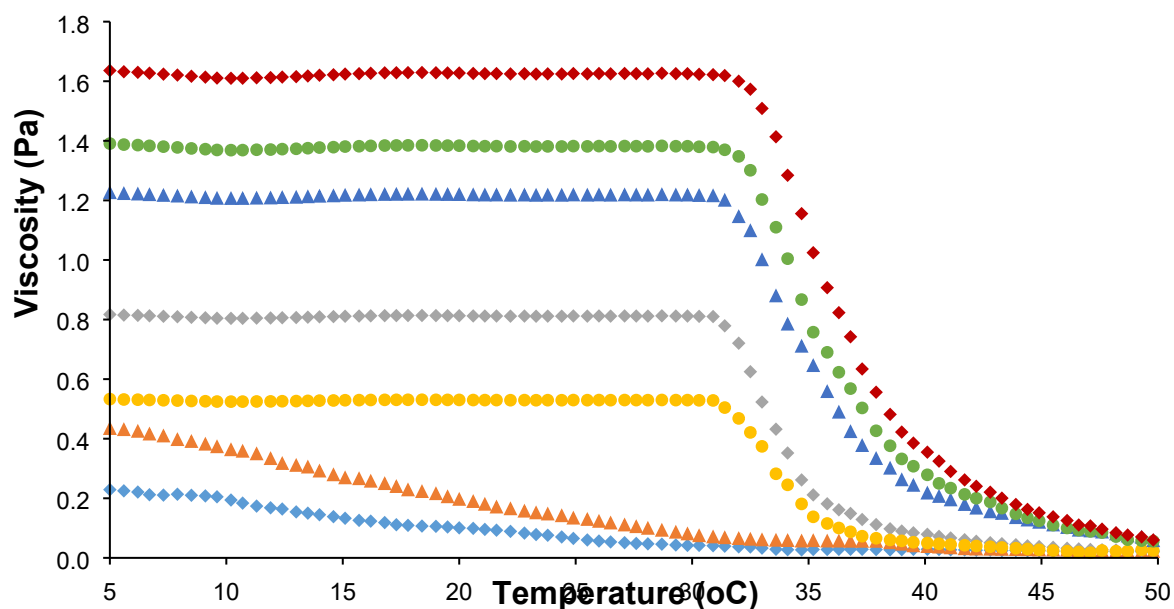


**Figure S22.** Measurements of the viscosity of aqueous samples of **C** at pH 8.5 ( $C^{3-}$ ) with increasing temperature: water (light blue  $\blacklozenge$ ), 0.25 wt%, 3.59 mmol, below CGC (orange  $\blacktriangle$ ), 0.5 wt%, 7.18 mmol at CGC (yellow  $\bullet$ ), 1 wt% 14.36 mmol (grey  $\blacklozenge$ ), 2 wt%, 28.72 mmol (dark blue  $\blacktriangle$ ), 3 wt%, 43.08 mmol (green  $\bullet$ ), 4 wt% 57.44 mmol (red  $\blacklozenge$ ).

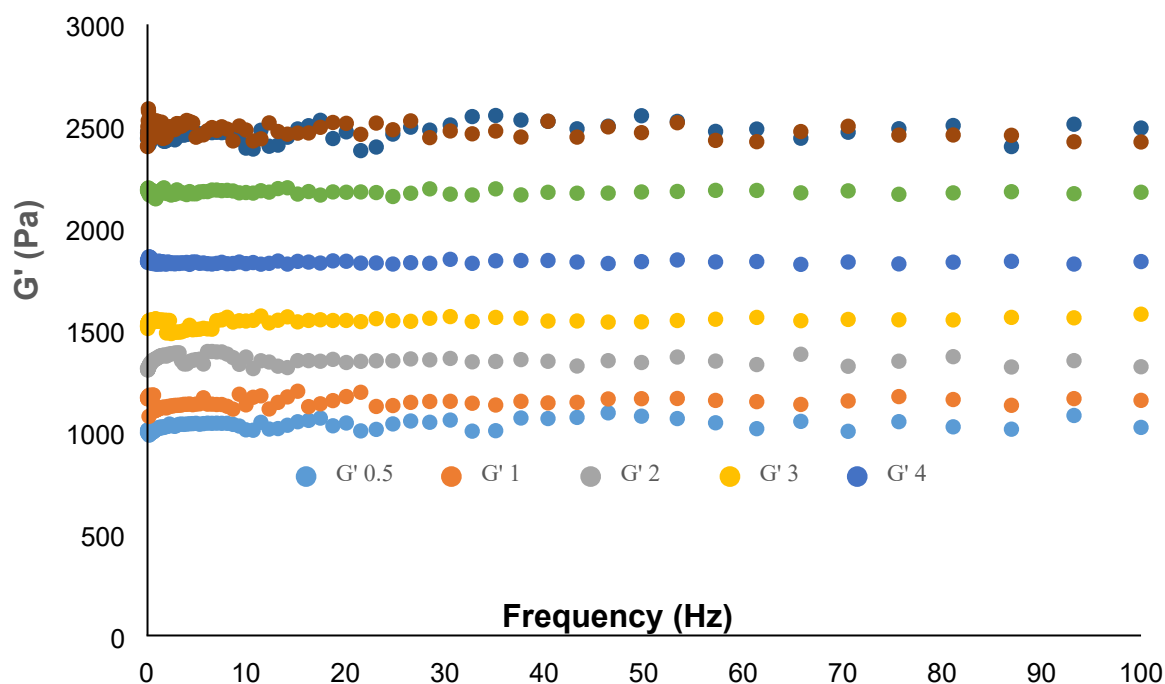


**Figure S23.** Frequency sweep experiments ( $G'$  shown) for the gels resulting from the set using a 2 ml portion of a 25 ml stock solution with a potential maximum  $C$  of  $28.2 \text{ mmol}^{-1}$  which was subjected to continuous mechanical agitation in the form of magnetic stirring at 1000 rpm.

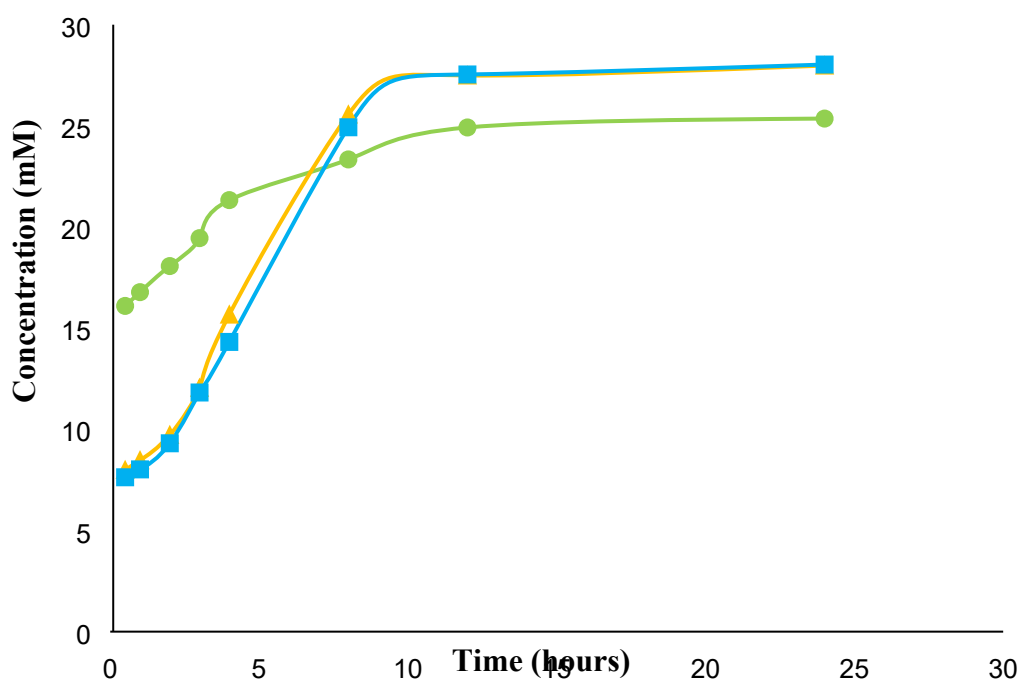


**Figure S24.** Concentration (in mM) of reaction product  $C^n-$  formed with a seed concentration of 1.5 mM, monitored over time by rheology (green  $\bullet$ ),  $^1\text{H}$  NMR (yellow  $\blacktriangle$ ) and HPLC (blue  $\blacksquare$ ) against time (hours, log scale) with a line added between data points to guide the eye.

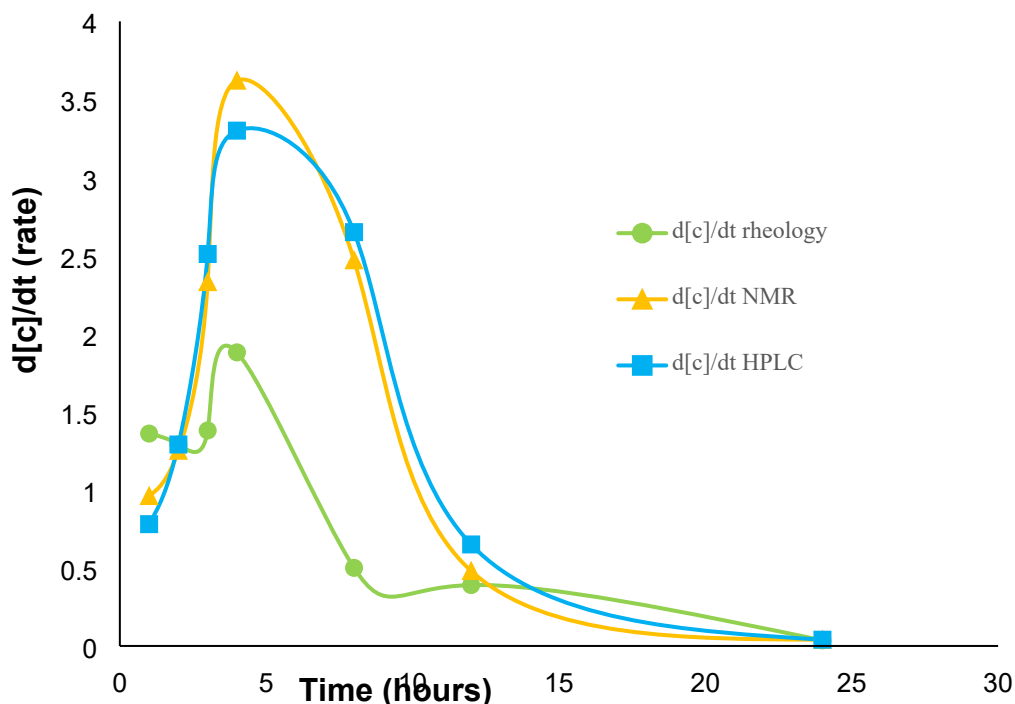


**Figure S25.** The rate of reaction of **A + B** to **C<sup>n-</sup>** calculated using the previously determined concentration from the by rheology (green ●), <sup>1</sup>H NMR (yellow ▲) and HPLC (blue ■) against time (hours, log scale) with a line added between data points to guide the eye.

## 13.0 standard vs seeding vs mechanical reaction conditions rate of reaction

Useful comparisons can be made between the rate of reaction associated with the three techniques used to control the reaction between **A** and **B** to form **C<sup>n-</sup>**. As can be seen in Figure S26, the reaction where the initial reaction mixture is seeded with *ex situ* prepared **C<sup>n-</sup>** shows the largest initial rate of reaction before decaying exponentially as **A** is rapidly consumed. This is due to the relatively large initial concentration of **C<sup>n-</sup>** acting as a catalytic species.

**Table S4.** Data for the rate of reaction for the formation of **C<sup>n-</sup>** as determined by HPLC analysis for the three methods used to control the rate of reaction (standard conditions, mechanical agitation and seeding).

time	d[c <sup>n-</sup> ]/dt mechanical	d[c <sup>n-</sup> ]/dt standard	d[c <sup>n-</sup> ]/dt seeded
1	0.78	0.12	3.50
2	1.29	1.44	5.41
3	2.51	2.60	5.85
4	3.30	2.51	2.92
8	2.65	1.43	0.57
12	0.65	0.91	0.27
24	0.04	0.25	0
48	0.00	0.04	0
72	0.00	0.02	0
96	0.00	0.00	0

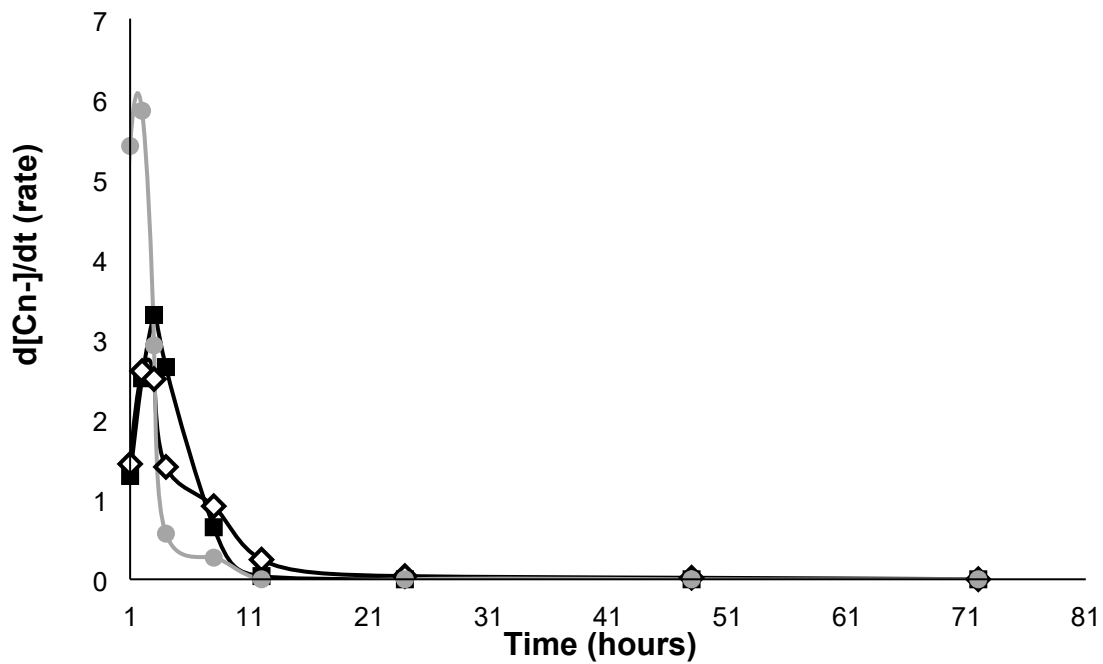


**Figure S26.** Rate of reaction plotted against time for each of the three techniques (standard conditions ◇, mechanical agitation ■, seeded ●) used to control the rate of reaction between **A** and **B** to form **C<sup>n-</sup>**.

## 14.0 Molar absorptivity determination for A and C

### 14.1 Molar absorptivity determination for A

The molar absorptivity ( $\epsilon$ ) of **A** could be determined by performing a concentration/absorption study with known concentrations of **A** in conjunction with the Beer-Lambert law ( $A_{bs} = \epsilon/c$ ).

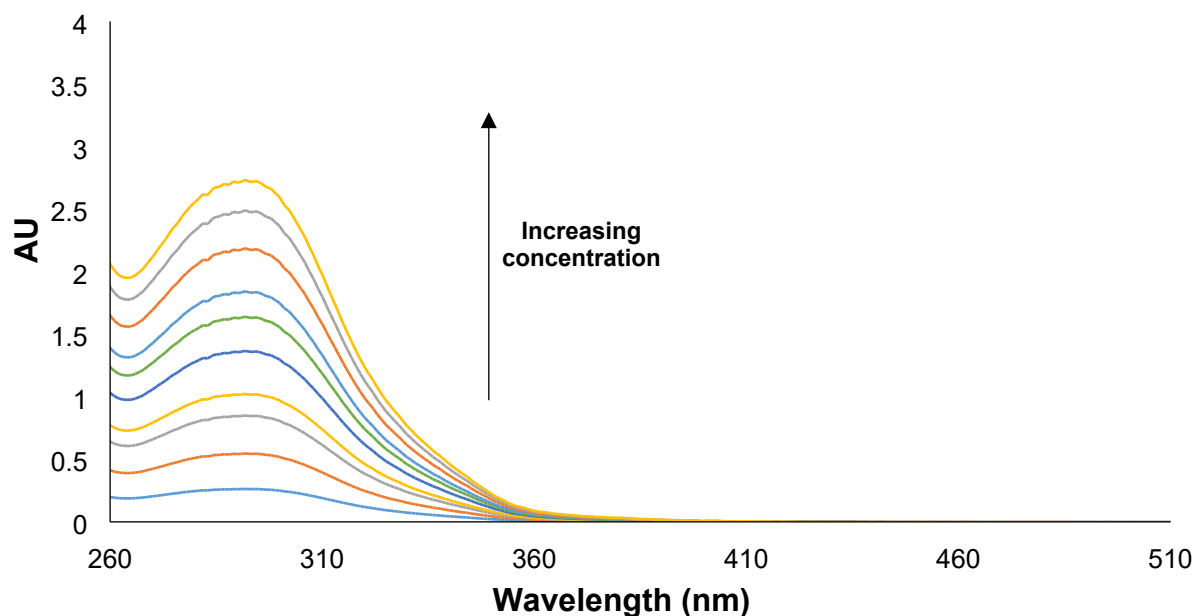


**Figure S27.** Concentration UV-vis absorption experiment for **A** using concentrations of: 4, 8, 12, 16, 20, 24, 28, 32, 36 and 40 mmol.

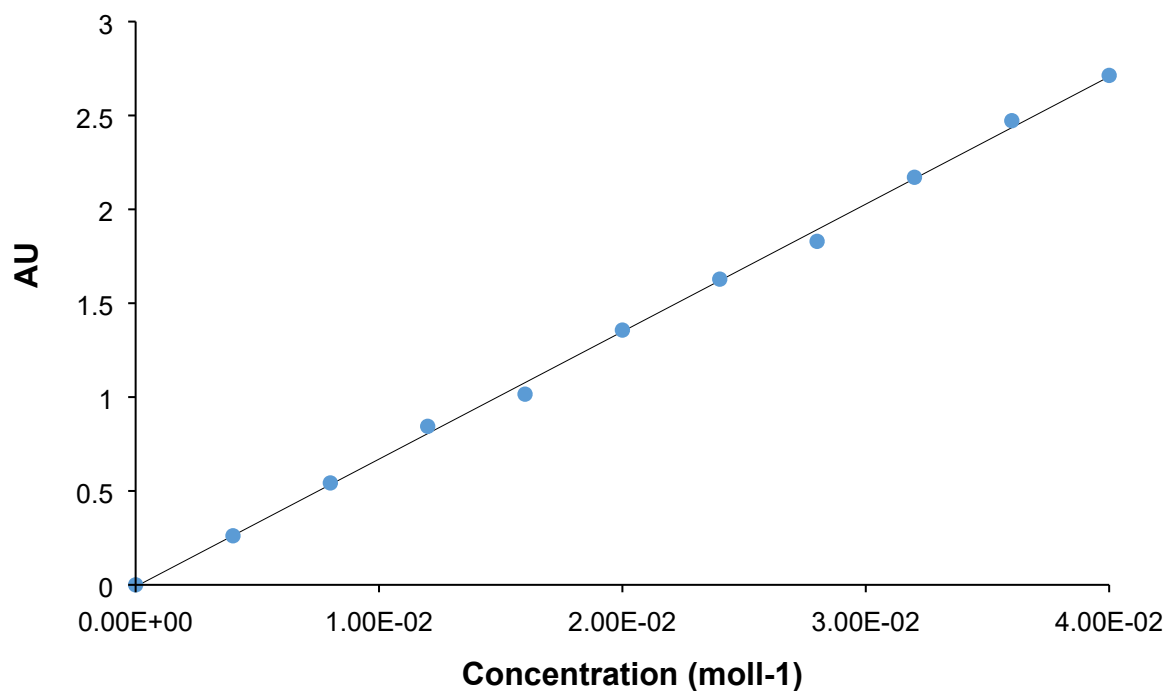


**Figure S28.** Determination of molar absorptivity ( $\epsilon$ ) for **A** at 290 nm by plotting the absorbance (AU) at 290 nm against each concentration.  $\epsilon$  is defined as the slope of the straight line.

## 14.2 Molar absorptivity determination for C

The molar absorptivity ( $\epsilon$ ) of **C** could be determined by performing a concentration/absorption study with known concentrations of **C** in conjunction with the Beer-Lambert law ( $A_{bs} = \epsilon/c$ ).

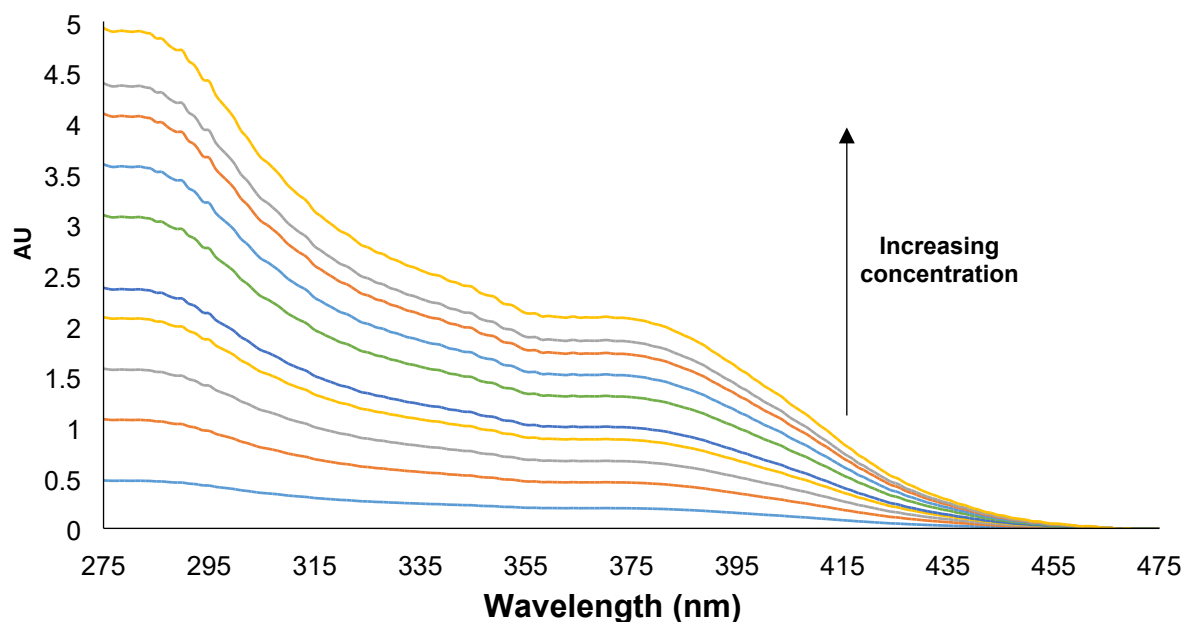


**Figure S29.** Concentration UV-vis absorption experiment for **C** using concentrations of: 4, 8, 12, 16, 20, 24, 28, 32, 36 and 40 mmol of an *ex situ* prepared sample of **C**.

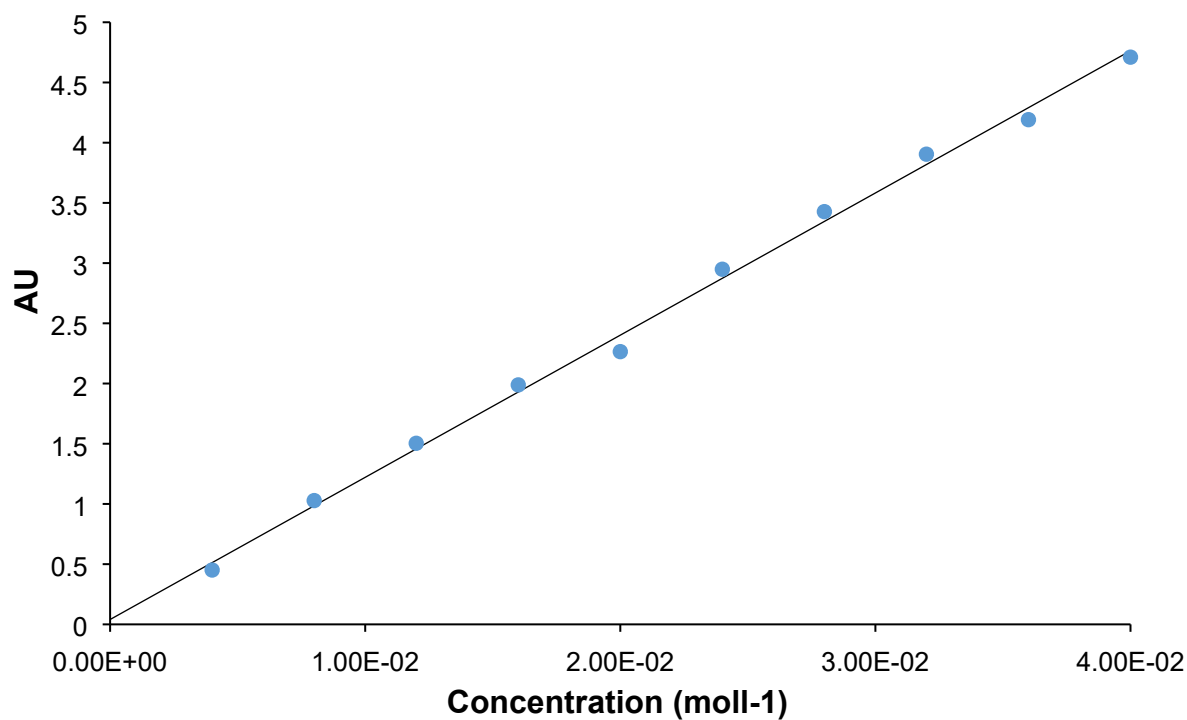


**Figure S30.** Determination of molar absorptivity ( $\epsilon$ ) for **C** at 290 nm by plotting the absorption (AU) at 290 nm against each concentration.  $\epsilon$  is defined as the slope of the straight line.

## 15.0 HPLC chromatograms for A and C

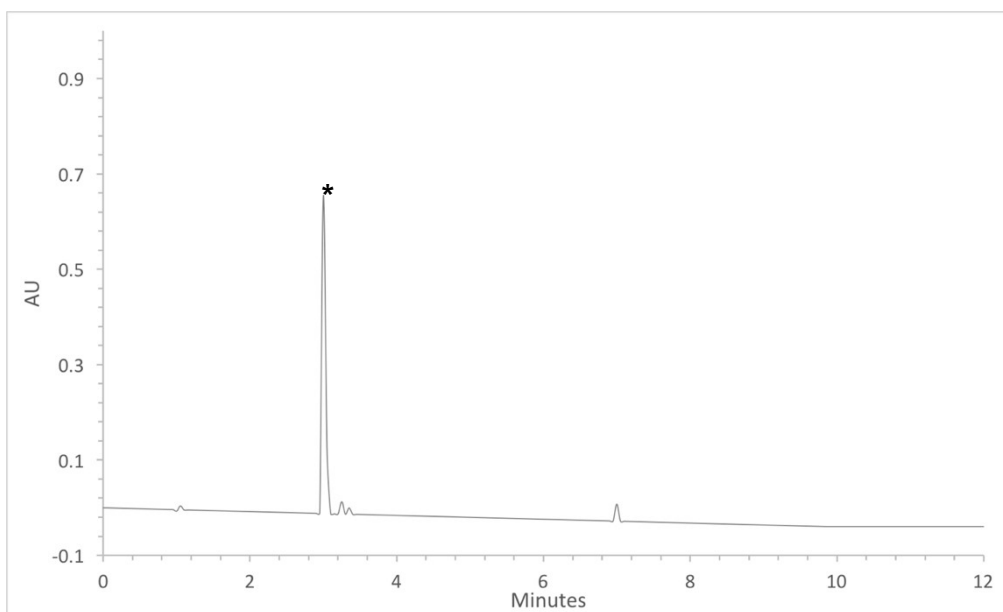


**Figure S31.** HPLC chromatogram (monitored at 290 nm) showing **A** (\*) with a retention time of 3 minutes 3 seconds.

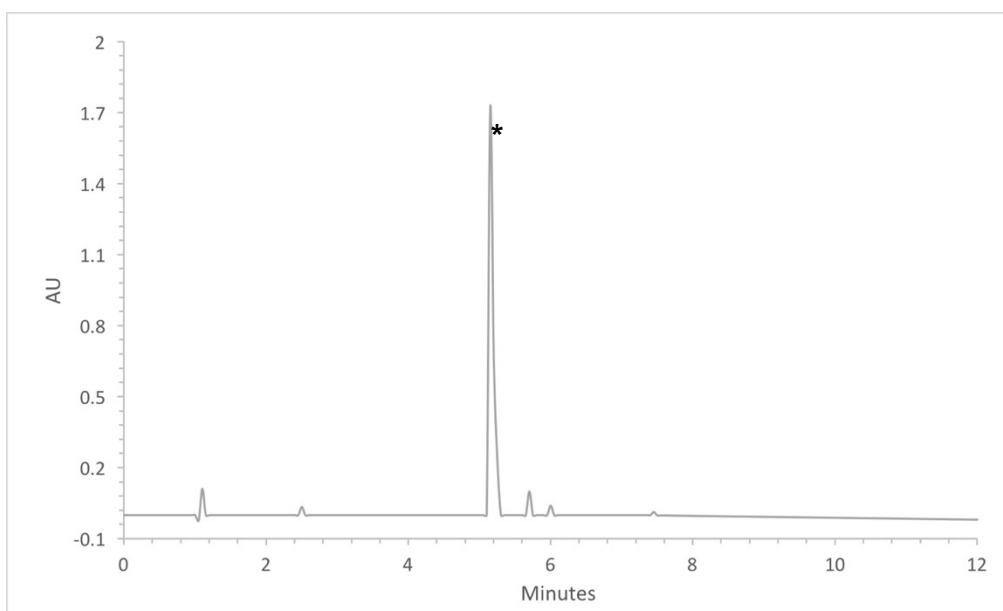


**Figure S32.** HPLC chromatogram (monitored at 290 nm) showing **C** (\*) with a retention time of 5 minutes 12 seconds.

## 16.0 HPLC data

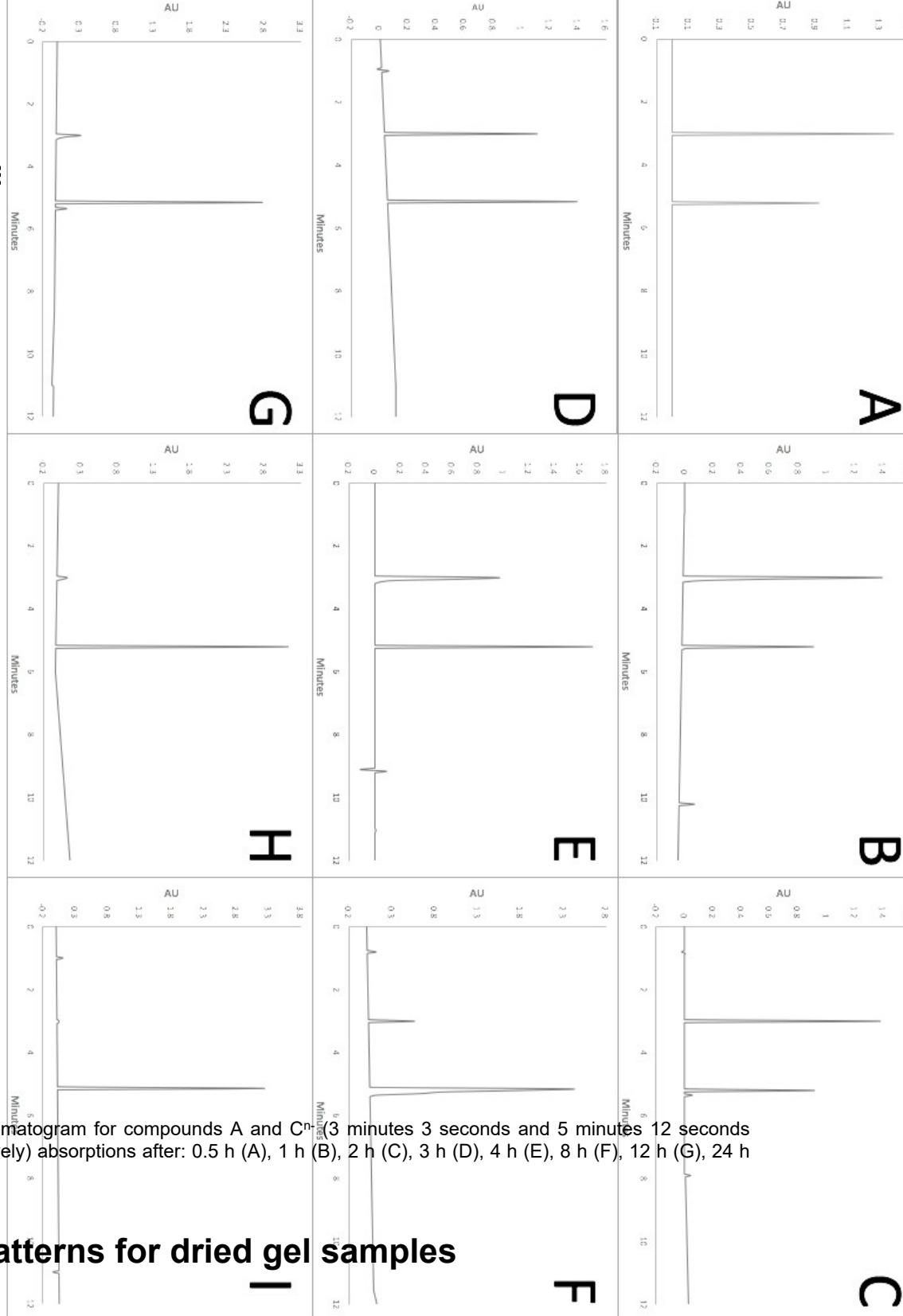


**Figure S33.** HPLC chromatogram for compounds A and C<sup>n</sup> (3 minutes 3 seconds and 5 minutes 12 seconds retention times respectively) absorptions after: 0.5 h (A), 1 h (B), 2 h (C), 3 h (D), 4 h (E), 8 h (F), 12 h (G), 24 h (H), 48 h (I).

## 17.0 PXRD patterns for dried gel samples

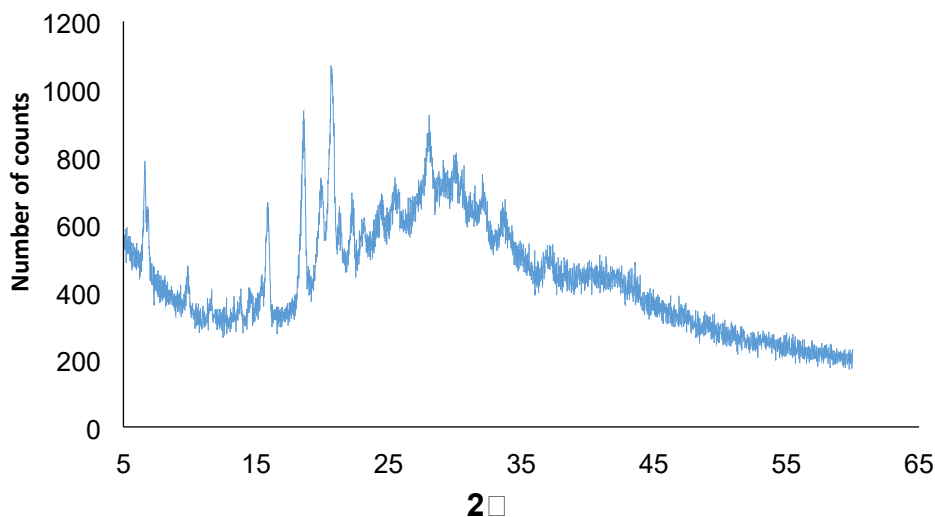


**Figure S34.** PXRD for *ex situ* prepared sample of **C** isolated after conversion to gel. Pattern obtained for an *ex situ* prepared sample of **C** that has been isolated from the gel by vacuum filtration. NMR experiment run after repeated washing with water (5 x 100 ml) in order to remove salts and gluconic acid sample was then oven dried overnight at 110 °C.

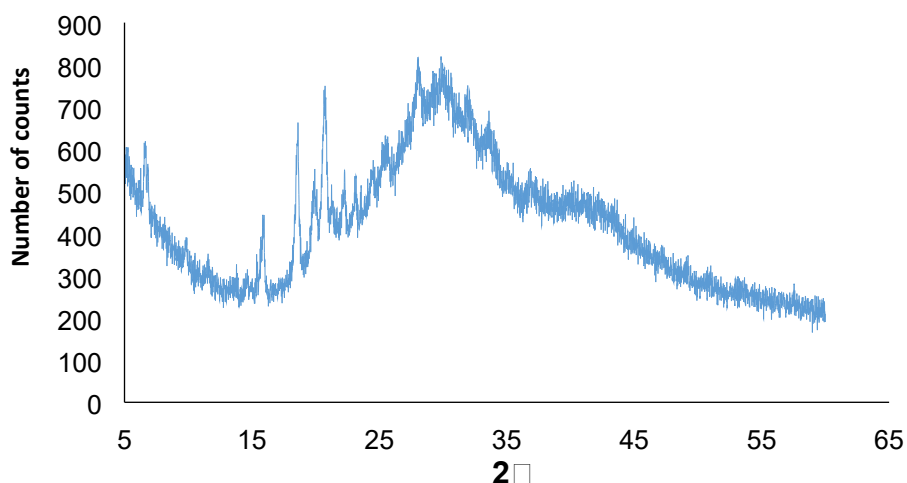


**Figure S35.** PXRD for *in situ* prepared sample of **C** isolated from gel. Pattern obtained for an *in situ* prepared sample of **C** that has been isolated from the gel by vacuum filtration. NMR experiment run after repeated washing with water (5 x 100 ml) in order to remove salts and gluconic acid sample was then oven dried overnight at 110 °C.

$\pi$ - $\pi$  stacking with the system was determined using the presented PXRD data. As can be seen in figures S34 and S35 there is a significant, broad reflection centered on a  $2\theta$  value of  $28.1^\circ$ . This corresponds to a distance of 3.3 Å which can be accounted for by  $\pi$ - $\pi$  stacking occurring between molecules of **C**.<sup>[1,2]</sup>

## 18.0 NMR spectra for C<sup>n-</sup>

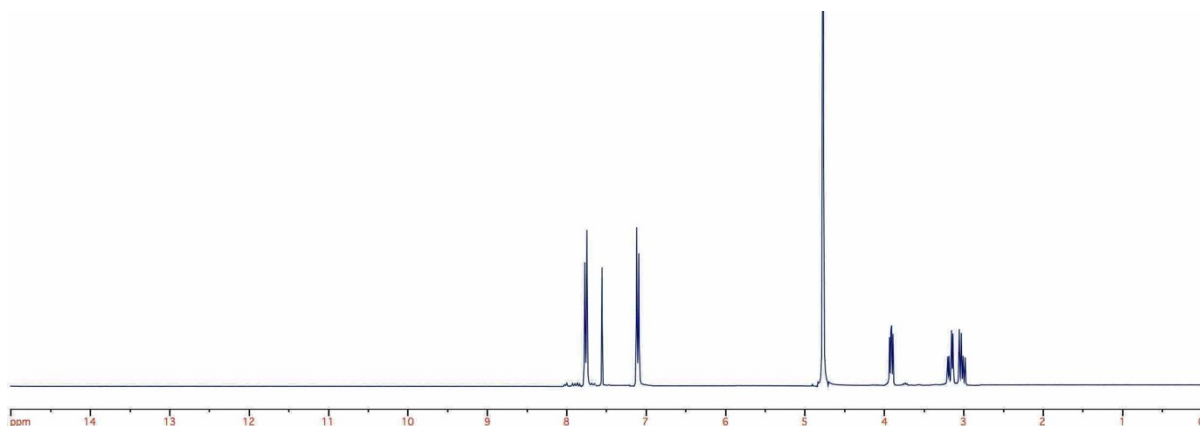


**Figure S35.** <sup>1</sup>H NMR spectra obtained for an *in situ* prepared sample of **C** that has been isolated from the gel by vacuum filtration. NMR experiment run after repeated washing with water (5 x 100 ml) in order to remove salts and gluconic acid sample was then oven dried overnight at 110 °C.

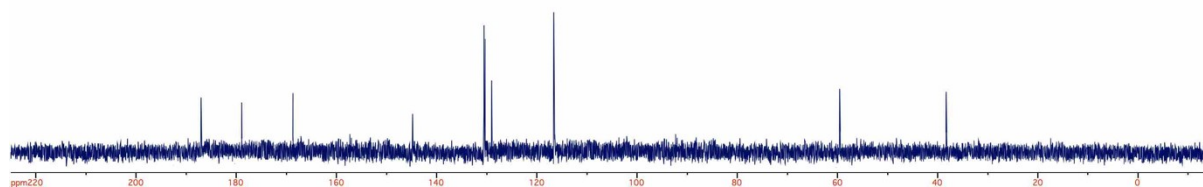


**Figure S35.** <sup>13</sup>C NMR spectra obtained for an *in situ* prepared sample of **C** that has been isolated from the gel by vacuum filtration. NMR experiment run after repeated washing with water (5 x 100 ml) in order to remove salts and gluconic acid sample was then oven dried overnight at 110 °C.

- [1] R. C. T. Howe, A. P. Smalley, A. P. M. Guttenplan, M. W. R. Doggett, M. D. Eddleston, J. C. Tan, G. O. Lloyd, *Chem. Commun.* **2013**, 49, 4268–70.
- [2] C. R. Martinez, B. L. Iverson, *Chem. Sci.* **2012**, 3, 2191.